Available online at www.sciencedirect.com
ScienceDirect
Transportation Research Part B 41 (2007) 722–735
TRANSPORTATION RESEARCH PART B
www.elsevier.com/locate/trb

Car following theory with lateral discomfort

Banihan Gunay *

Transport and Road Assessment Centre, Faculty of Engineering, University of Ulster, BT37 0QB, Co. Antrim, UK

Received 10 October 2005; received in revised form 7 August 2006; accepted 12 February 2007

Abstract

A car following model has been developed with particular reference to weak discipline of lane-based driving. The theory is based on the discomfort caused by lateral friction between vehicles. The movement of the following vehicle was formulated as a function of the off-centre effects of its leader(s). This incorporation of lateral friction offers a potential breakthrough in the fields of car following theory and microscopic simulation of traffic flow. Using a stopping-distance car following approach, the simulation presented in the paper pointed out the effect of the travel path width on the speed of the following vehicle, and the reduced following distance with increased lateral separation between the leader and follower. It was also shown that a special case of the proposed model (i.e. when the maximum escape speed is zero) produced the same results as the base model did for the conventional car following case. The simulation behaved rationally giving credibility to the author's staggered car following theory.
© 2007 Elsevier Ltd. All rights reserved.

Keywords: Car following; Lane discipline; Lane-based driving; Lateral position of traffic

1. Introduction

The key assumptions of car following theory state that vehicles travel in the middle of the lane, each vehicle is influenced directly by the one in front, and no passing is allowed. From qualitative observations of any road traffic, however, it is not difficult to notice that not every vehicle is positioned in the centre of the lane. These deviations from the centre become considerable especially in places where non-lane-based driving is predominant (the term will be defined later in this section). Best examples of this kind are from developing countries where poor road surface and markings as well as irregular driver attitudes are the reasons behind the problem (Khan and Maini, 1999; Gunay, 2004). Even in developed countries, lateral friction may play a role in car following or passing behaviour, unless the lanes are clearly separated by road markings with good visibility, lane widths are wide enough, and drivers have perfect driving discipline.

Case et al. (1953) stated that drivers veered around objects near their path located on the roadside, and reacted to curbing height, shoulder width, lane width, centre line, and variations in pavement surface. In a

* Tel.: +44 2890366022; fax: +44 2890366826.
E-mail address: b.gunay@ulster.ac.uk

0191-2615/$ - see front matter © 2007 Elsevier Ltd. All rights reserved.
doi:10.1016/j.trb.2007.02.002

similar study, Taragin (1955) reported that depending on the size and distance of the objects from the carriageway platform, some drivers encroached on the lane used by oncoming traffic in two-lane two-way highways. He found that as the flow increased on a two-lane unidirectional highway, vehicles in the shoulder lane, on an average, travelled closer to the shoulder, and those in the median lane travelled closer to the median. May (1959) introduced four types of friction as internal, medial, marginal, and intersectional. Internal friction was defined as that friction which exists between vehicles moving in the same direction. He outlined the possible factors influencing the internal friction, such as number and width of lanes, horizontal and vertical alignment, and uniformity and smoothness of traffic flow. Nevertheless, there was no further elaboration on mathematical representation of internal friction in his paper. Later, Michales and Cozan (1963) investigated the relationship between the speed of a vehicle and lateral clearance, stating that it was possible, when necessary, to control the speed of traffic by means of a channel constructed by plastic cones. The width of this channel and the longitudinal distances between each consecutive cone are the factors affecting the speed of traffic. Mahalel (1984) developed a simulation model to evaluate the quality of traffic flow. His evaluation was based on the number of potential speed changes and the number of times a vehicle is limited in changing lanes. But two-dimensional car following concept was not treated. Refer to Martens (1997) who provided a detailed review on the effects of road design on speed behaviour.

Gunay (2003) defined the term lane-based driving discipline as the tendency to drive within a lane by keeping to the centre as closely as possible (unless in lane changing), and introduced four possible scales to quantify this discipline. Irregular distribution of traffic across the roadway was the most important indications of weak discipline. For example, central positions of vehicles were recorded in Germany (Fig. 1a) and these vehicles positioned themselves laterally within their lanes according to a normal distribution. When similar analyses were carried out for the data collected from Turkey, his findings exhibited less tidy distribution where some vehicles travelled over the lane lines or even on the shoulder (Fig. 1b). He categorised traffic flow into tidy and untidy depending on whether the lateral distribution of vehicles fits a normal curve or not. He summarised defining characteristics of weak discipline of lane-based driving as: (a) irregular lateral position of vehicles across the carriageway; (b) driving on lane lines for long time; (c) usage of the shoulder as a traffic lane; (d) when lateral clearance is restricted speeds may be affected, and (e) shorter following headways with more central separations between two consecutive vehicles.

Three sets of data, collected earlier for another piece of research, were analysed to see the characteristics of varying lane discipline. Sites were straight sections of multilane highways with uninterrupted traffic flows on A167(M), Newcastle, Britain; A5-Bruchsal, Karlsruhe, Germany; and a number of different sites (mainly on E5, Atakoy), Istanbul, Turkey. It was revealed that the overtaking vehicles laterally located themselves with respect to the lateral position of the vehicle being overtaken (Fig. 2). Regarding the relationship between side clearance, i.e. frictional clearance (FC in Fig. 2), and the overtaking speeds, speeds of passing vehicles remained unchanged in tidy flows as long as vehicles do not encroach on the adjacent lanes. Untidy traffic, however, exhibited a different picture, as Fig. 3 shows two examples. Both graphs suggest some increase in

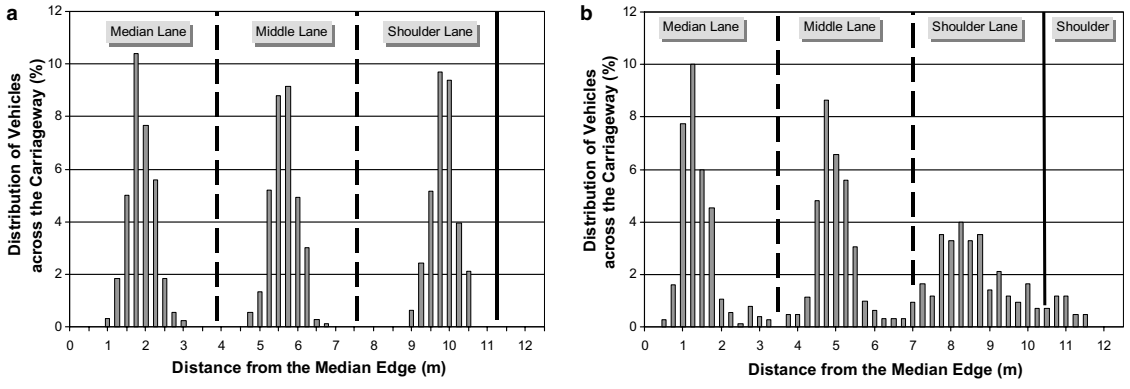

Fig. 1. Demonstration of good and poor disciplines of lane-based driving. Adapted from Gunay (2003).

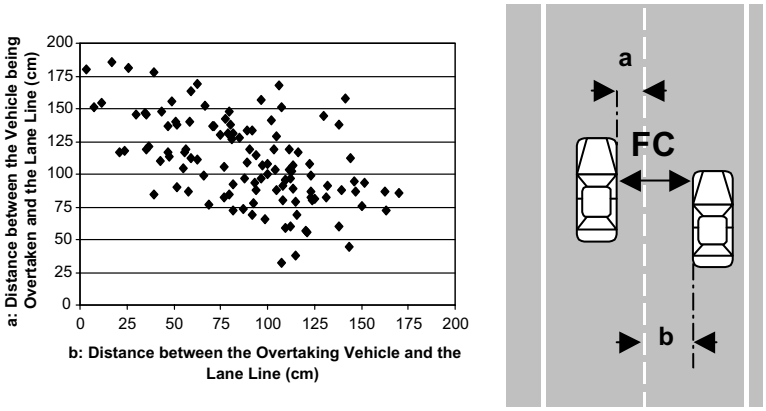

Fig. 2. Lateral discomfort of the neighbouring vehicle on a two-lane carriageway.

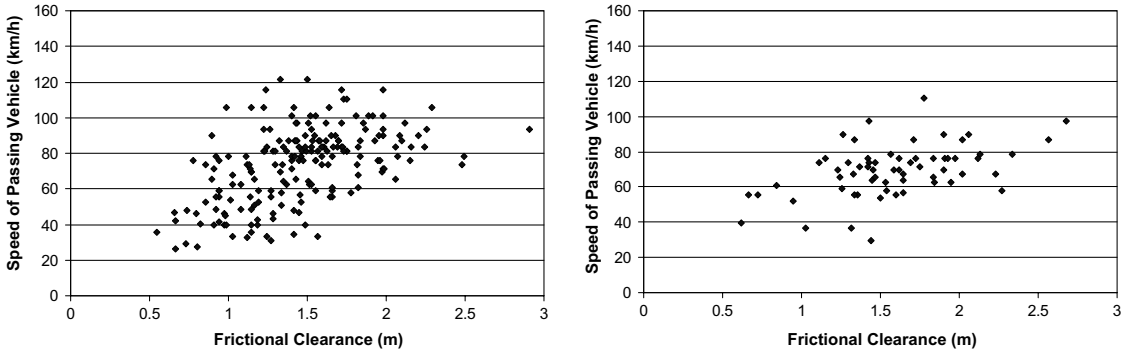

Fig. 3. The relationship between frictional clearance and passing speed at two different locations.

the speeds of passing vehicles with increasing FC available. Further analysis of the data were undertaken to find if there is any relationship between the lateral separation of the two consecutive vehicles and the time headway between them. The findings did not show any clear correlation between these two characters for Britain and Germany, because CS (shown in Fig. 4) never became large enough. But the data form Turkey suggested a decline in the following headways (Fig. 5). This shows that vehicles tend to keep shorter headways when there is some horizontal separation between them. Other data sets of his work, collected from various sites revealed very similar trends.

Finally, to sum up and conceptualise the phenomenon, consider the following scenarios. Highway standards recommend that the nearest roadside object or a traffic sign must be located some distance away from

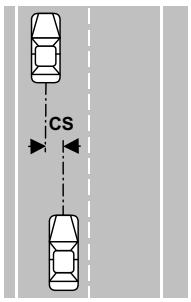

Fig. 4. Depiction of a typical staggered car following situation, where CS is the centreline separation between the two consecutive vehicles.

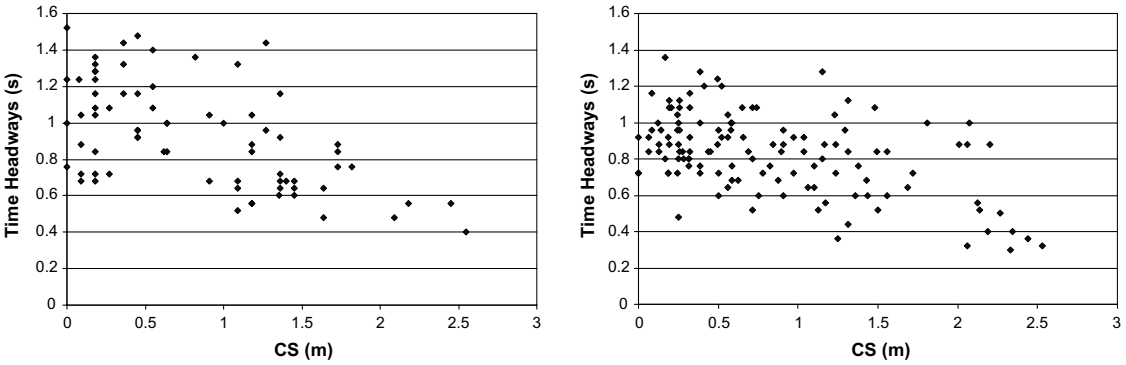

Fig. 5. Time headways vs. lateral separation of two consecutive vehicles in Turkey, on two different locations.

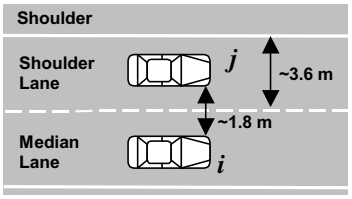

Fig. 6. A typical motorway geometry producing minimal lateral discomfort.

the edge of the carriageway (Highway Capacity Manual, 2000), so that psychologically drivers are not affected by the objects and they do not swerve along. Assuming an optimum side clearance of about 1.8 m, as they recommend, and an average vehicle width of 1.8 m, shown in Fig. 6, two boundary conditions exist for an ideal case where vehicles can be located on any horizontal position within their lanes: (a) when ***j*** travels on the left-hand side of the shoulder lane, ***i*** can approach to the lane line as much as possible; and (b) when ***j*** travels on the right-hand side of the shoulder lane, ***i*** has to keep a comfortable lateral clearance to ***j*** (i.e. ***i*** is probably now on the right-hand side of the median lane). These boundary conditions show that as long as ***j*** does not occupy the adjacent lane, ***i*** has the freedom of 1.8 m (maximum) lateral displacement. In other words, ***i*** can overtake[1] ***j*** and maintain the current speed by making the necessary lateral displacement, rather than reducing the speed. After this point, every bit of encroachment of the median lane by ***j*** will make ***i*** reduce the speed to eliminate the lateral discomfort (or even abandon the overtaking), since there is no longer room for any lateral displacement for ***i*** towards the right. This freedom of making use of the lateral space may sometimes be not available where the neighbouring vehicle is a heavy vehicle.

2. Basic (conventional) car following – a brief review

Research on car following theory dates back to the mid 20th century. Forbes (1963) found that the reaction time needed for the following driver to perceive the necessity to decelerate and apply the brakes is the key factor. Thus, a minimum safe (time) headway should at least be the sum of the reaction time and the time required for the leading vehicle to traverse a distance which is equal to its length. Pipes (1966) characterised the suggestion of the California Motor Vehicle code as "a good rule for following another vehicle at a safe distance is to allow yourself at least the length of a car between your vehicle and the vehicle ahead for every 10 miles per hour of speed at which you are travelling". It is clear that Forbes' and Pipes' theories give a linear increase of the minimum safe distance headway with increasing speed. The research team of the General Motors (GM) Company (reviewed by May, 1990) produced five generations of their car following models

[1] For simplicity, the terms "overtaking" and "passing" are used interchangeably throughout the paper, although they are slightly different.

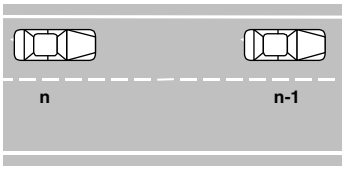

Fig. 7. Basic (tidy) car following. For the formulations throughout the paper, the symbols 'n' and '$n-1$' will represent the following and leading vehicles, respectively. Vehicle 'n' will always be the subject vehicle, which is the subject of the update procedure of the simulation as will be shown later in the paper.

which were all based on an analogy that the response of the following driver (acceleration or deceleration) is a function of the sensitivity of this driver and the stimulus. This stimulus is generally the relative speed between the two vehicles. Gipps (1981) proposed a model with parameters that correspond to obvious characteristics of drivers and vehicles so that most can be assigned values without resorting to elaborate calibration procedures, and his model behaved well when the interval between successive recalculations of speed and position is the same as the reaction time, that is also what is done in the widely used Nagel-Schreckenberg cellular automata model (Nagel and Schreckenberg, 1992). There are many more car following models available in the literature, in addition to the above summary. Each model has certain advantages and disadvantages. For a broader review, refer to Holland (1998) and Brackstone and McDonald (1999). To conclude, car following theory can be categorised in two groups: stimulus based (or psycho-psysical) models, e.g. GM models; and stopping-distance based (or safety distance) models, e.g. Gipps' model. For some researchers, further categories, i.e. action-point models (Leutzbach and Wiedemann, 1986) and cellular automata models (Daganzo, 2006) can also be mentioned.

For the present paper, to start with, a stopping-distance based approach has been employed, resulting in the author's non-lane-based car following model, also known as a staggered car following model. Adaptations of other well-known car following models to the issue of non-lane-based driving discipline will follow as on going work. In a basic follower–leader interaction (Fig. 7), according to the stopping-distance based approach, the speed of the following vehicle at the end of the reaction time is calculated as in (1), the derivation of which can be found in Gipps (1981). The longitudinal location of the following vehicle is updated with respect to this new speed value.

$$v_n(t+\tau) \leqslant b_n\tau + \sqrt{b_n^2\tau^2 - b_n\left\{2[y_{n-1}(t) - s_{n-1} - y_n(t)] - v_n(t)\tau - \frac{[v_{n-1}(t)]^2}{\widehat{b}}\right\}}, \tag{1}$$

where $v_n(t+\tau)$ is the speed of the following vehicle at time $(t+\tau)$; b_n is the deceleration rate of the following vehicle; τ is the reaction time; $y_{n-1}(t)$ is the position of the leading vehicle at time t; s_{n-1} is the length of vehicle $n-1$ including the stationary stoppage allowance; $y_n(t)$ is the position of the following vehicle at time t; $v_n(t)$ is the speed of the following vehicle at time t; $v_{n-1}(t)$ is the speed of the leading vehicle at time t; and $\widehat{b}$ is the perceived (by the following driver) deceleration of the leading vehicle, and will be assumed to be the same as b_{n-1} throughout the paper for simplicity, where b_{n-1} is the deceleration rate of the leading vehicle.

3. Involvement of lateral discomfort in car following

In non-lane-based car following, because of the off-centred positions of vehicles, the following driver does not assign leadership fully to the vehicle most in front. That is to say, when the primary leader starts suddenly to decelerate at time t, and stops eventually, the vehicle behind responds to this stimulus τ s later as in lane-based following, explained in Section 2. But, at the same time, the following driver, instead of stopping just behind the leading vehicle, considers (laterally) shifting his/her vehicle towards the space beside the leader. The aim of the following driver is now to avoid a rear-end collision by using this escape corridor. Then, unlike basic car following, the follower's speed does not need to be reduced to zero. In other words, whereas in the basic car following case (Eq. 1), both vehicles stop, in the non-lane-based (staggered) car following case, the following driver may have the opportunity to shift and pass the (stopped) leader. Hence, the maximum

allowed speed is now determined by the most restrictive of two factors: (a) a speed at which the vehicle can decelerate (at time of passing) to the maximum speed allowed by the width of this escape corridor; and (b) a speed which should allow the following vehicle adequate time to veer laterally so as to safely avoid a rear-end collision. The former will be called maximum escape speed (MES) and be used in the first part of the modelling. "t_{veer}" (veering time) will form the latter factor and be used in the second part (see also Figs. 10 and 11). Therefore, the following distance between the two consecutive vehicles is a function of the width of the escape route and the amount of off-centredness between them. Fig. 8 demonstrates an approximate shape of this relationship.

For better understanding, Fig. 9 summarises the dynamic nature of the interaction. In the first depiction, maximum escape speed (MES) is smaller than the speed of the leading vehicle and therefore is not enough for the follower to perform a passing. The following distance at a given time is shorter than that of a basic car following case. In the second depiction, however, the speed of the following vehicle, not necessarily constant, is greater than the leader's speed, and the speed of the leader is smaller than MES allowed by the width of the corridor on one side of the leading vehicle. The follower approaches to the leader, realises the speed difference between them, and decides to pass the leader. But the speed of this passing is limited by MES.

Assuming a carriageway with standard lane and shoulder widths, drivers will only be able to maintain the design speeds where they have enough lateral clearance on both sides of their vehicles. The new car following model will assume that the speed of a vehicle is affected by the width of the travel path, i.e. the effective route

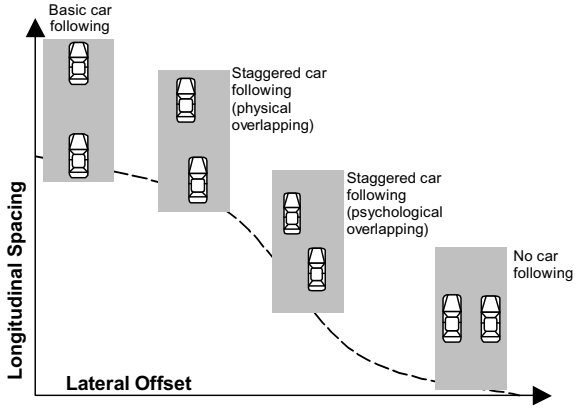

Fig. 8. A typical trend of the relationship between horizontal separations of the two consecutive vehicles and the following distance between them.

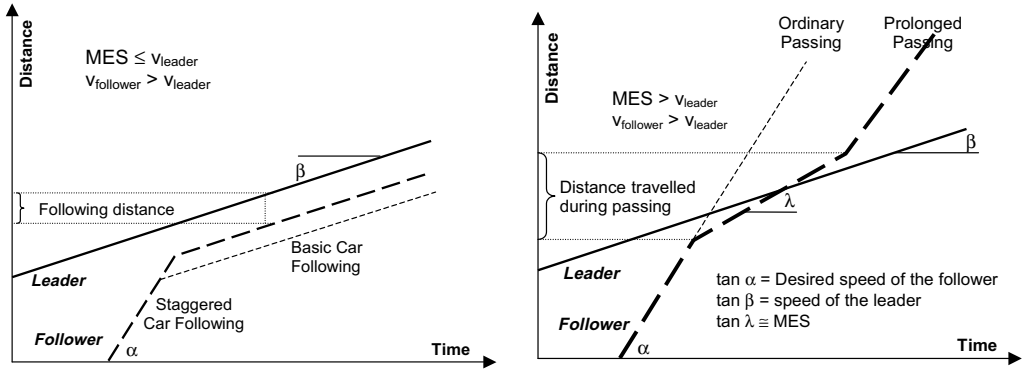

Fig. 9. Typical space–time diagrams of two different staggered car following cases, where the follower eventually passes the leader in the second depiction. Linearisation of the curves is only to simplify the demonstration.

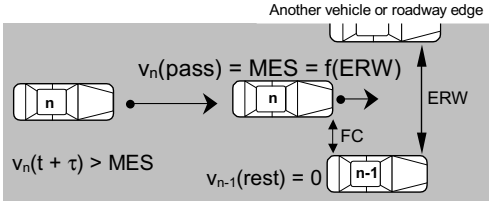

Fig. 10. MES governed following in non-lane-based traffic.

width (ERW) in Fig. 10. Fig. 3 had implied that with large values of frictional clearance (FC), the effect of the adjacent vehicle on the passing vehicle was not noticeable. In the formulation, the FCs on both sides of the vehicle are assumed to be the same, as vehicles generally tend to travel at the centre of their travel path in the real world.

From dynamics, the interaction between the two vehicles can be expressed as:

$$y_n(\text{pass}) = y_n(t) + \frac{v_n(t) + v_n(t+\tau)}{2}\tau - \frac{\text{MES}^2 - v_n^2(t+\tau)}{2b_n}, \tag{2}$$

where y_n(pass) is the longitudinal location of the following vehicle when it commences passing the (stopped) off-centre leader. The last term, i.e. $-\frac{\text{MES}^2 - v_n^2(t+\tau)}{2b_n}$, is explained in Appendix A. The rest of the symbols were stated in Section 2. For safe following, $y_{n-1}(\text{rest}) - s_{n-1}$ should be greater than y_n(pass), as shown in (3).

$$y_{n-1}(t) - \frac{v_{n-1}^2(t)}{2b_{n-1}} - (s_{n-1}) \geqslant y_n(t) + \frac{v_n(t) + v_n(t+\tau)}{2}\tau - \frac{\text{MES}^2 - v_n^2(t+\tau)}{2b_n}. \tag{3}$$

By introducing a safety margin, $\{v_n(t+\tau)\}\theta$, for possible errors of driver n, where θ is given as $\frac{\tau}{2}$ by Gipps (1981), (3) can be rewritten as in (4).

$$y_{n-1}(t) - \frac{v_{n-1}^2(t)}{2b_{n-1}} - s_{n-1} \geqslant y_n(t) + \frac{v_n(t) + v_n(t+\tau)}{2}\tau + v_n(t+\tau)\frac{\tau}{2} - \frac{\text{MES}^2 - v_n^2(t+\tau)}{2b_n}, \tag{4}$$

where $b_n < 0$ and $b_{n-1} < 0$. By rearranging this, (5) is obtained.

$$-\frac{v_n^2(t+\tau)}{2b_n} + \tau v_n(t+\tau) + \frac{\tau}{2}v_n(t) + \frac{\text{MES}^2}{2b_n} + \frac{v_{n-1}^2(t)}{2b_{n-1}} + y_n(t) - y_{n-1}(t) + s_{n-1} \leqslant 0. \tag{5}$$

This quadratic inequality is in the form of $\alpha x^2 + \beta\, x + \gamma \leqslant 0$, where

$$\alpha = -\frac{1}{2b_n},$$
$$\beta = \tau,$$
$$\gamma = \frac{\tau}{2}v_n(t) + \frac{\text{MES}^2}{2b_n} + \frac{v_{n-1}^2(t)}{2b_{n-1}} + y_n(t) - y_{n-1}(t) + s_{n-1}, \quad \text{and}$$
$$x = v_n(t+\tau).$$

The two roots of this inequality can be calculated by $\frac{-\beta \mp \sqrt{\beta^2 - 4\alpha\gamma}}{2a}$. Since we are not interested in minus speed values, the speed of the following vehicle at the end of the reaction time should be

$$v_n(t+\tau) \leqslant b_n\tau + \sqrt{(b_n\tau)^2 + 2b_n\left\{v_n(t)\frac{\tau}{2} + \frac{\text{MES}^2}{2b_n} + \frac{v_{n-1}^2(t)}{2b_{n-1}} + y_n(t) - y_{n-1}(t) + s_{n-1}\right\}}. \tag{6}$$

This is the maximum speed that the following vehicle should not exceed at the end of the reaction time, in order to maintain the required safe following distance. In short, the wider the escape route, the higher the MES, and hence the shorter the minimum safe following distance required, with higher values of $v_n(t+\tau)$. An illustrative example is given in Appendix B to test the accuracy of this formulation. The selection of con-

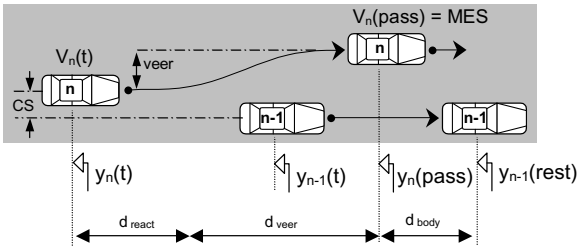

Fig. 11. Partial lane change, based on a required lateral clearance rather than lane-based switches.

crete values within the range permitted by this inequality for use in a possible simulation model can be made simply by assuming it as an equation. The improvement of this assumption was left for further study. It is interesting to note that when MES equals zero, (6) yields the same results as (1). This important feature of the model holds and is proven in Appendix C.

A further consideration is needed especially where the amount of the lateral shift is significant, as demonstrated in Fig. 11. That is the time needed to shift the vehicle in order to avoid a collision, even if the width of the escape route is wide enough. This is not an extra distance to be added to the existing following distance which was formulated by (6), because, for simplicity, it is assumed that the following driver can perform a slowing down and a lateral shift at the same time.

For a safe passage beside the leader, the following criterion should be met

$$y_{n-1}(\text{rest}) - y_n(t) \geqslant d_{\text{react}} + d_{\text{veer}} + d_{\text{body}}, \tag{7}$$

where

$d_{\text{react}} = \frac{v_n(t)+v_n(t+\tau)}{2}\tau$, i.e. the distance travelled during reaction time,

$d_{\text{veer}} = v_n(t+\tau)t_{\text{veer}} - \frac{1}{2}b_n(t_{\text{veer}})^2$, i.e. the distance travelled during the veering manoeuvre possibly with some slowing down. This term may be too small and could be neglected but the discussion of this is left for future research.

$b_n = \frac{v_n(t+\tau)-\text{MES}}{t_{\text{veer}}}$ or $b_n = -\frac{\text{MES}-v_n(t+\tau)}{t_{\text{veer}}}$ for convenience, and $t_{\text{veer}} = \frac{\text{veer}}{V_{\text{veer}}}$, where veer is the amount of lateral shift, and V_{veer} is the maximum lateral manoeuvring speed that can be obtained from manufacturers' vehicle specifications.

After the substitutions, we can write

$$\frac{v_n(t)+v_n(t+\tau)}{2}\tau + v_i(t+\tau)t_{\text{veer}} + \frac{1}{2}\frac{\text{MES}-v_n(t+\tau)}{t_{\text{veer}}}t_{\text{veer}}^2 + d_{\text{body}} \leqslant y_{n-1}(\text{rest}) - y_n(t). \tag{8}$$

By rearranging (8) to yield (9) as

$$\frac{\tau}{2}v_n(t+\tau) + t_{\text{veer}}v_n(t+\tau) - \frac{t_{\text{veer}}}{2}v_n(t+\tau) \leqslant y_{n-1}(\text{rest}) - y_n(t) - \frac{v_n(t)}{2}\tau - \frac{t_{\text{veer}}}{2}\text{MES} - d_{\text{body}}, \tag{9}$$

we obtain (10).

$$\left[\frac{\tau}{2} + t_{\text{veer}} - \frac{t_{\text{veer}}}{2}\right]v_n(t+\tau) \leqslant y_{n-1}(\text{rest}) - y_n(t) - \frac{v_n(t)}{2}\tau - \frac{t_{\text{veer}}}{2}\text{MES} - d_{\text{body}}. \tag{10}$$

Then the speed of the follower at the end of the reaction time should not exceed (11), in order to be able to perform the required veering manoeuvre. Namely, the bigger the 'veer' value, the longer the safe following distance.

$$v_n(t+\tau) \leqslant 2\frac{y_{n-1}(\text{rest}) - y_n(t) - \frac{v_n(t)}{2}\tau - \frac{t_{\text{veer}}}{2}\text{MES} - d_{\text{body}}}{t_{\text{veer}} + \tau}. \tag{11}$$

In short, whereas (1) represents a conventional car following model, (6) or (11) form the new dimensions. In a possible application of the proposed model, a simulation program should update the speed of the following vehicle according to these formulae, whichever governs the situation.

4. The simulation

4.1. The mechanism

A computer program in C++ language has been developed to simulate the above models. First of all, the current maximum escape speed (MES) is calculated as a function of frictional clearance (FC). If FC is smaller than 0.5 m, then MES is assumed to be zero, since with FC values less than 0.5 m, the use of the escape corridor was not practical (remember taking MES as zero, gives the same results of tidy following). If FC is between 0.5 and 1.5 m, the data shown in Fig. 3a is used. The program picks the corresponding speed value for a given current FC by fitting a second order curve to the plots, the equation of which is shown in (12), with $R^2 = 0.35$. Obviously, seeking a better fit, or finding another curve (or line) with more data given would change the formulation of MES, but this was left for future refinement of the simulation.

$$\mathrm{MES} = -17.2(\mathrm{FC})^2 + 77.6(\mathrm{FC}) - 0.7 \ldots 0.5 < \mathrm{FC} < 1.5 \tag{12}$$

If FC is greater than 1.5 m, it is assumed that the effect of the neighbouring vehicle is negligible, and thus, MES is taken as the same as the subject vehicle's current speed, $v_n(t)$. Namely, the subject vehicle's (i.e. the follower) movement is not restricted by any staggered leader. This value is arbitrarily assumed, by visual inspection of Fig. 3, to test the validity of the proposed model in the simulated environment and left as potential topics for future research.

Then, four different speeds with various constraints are calculated. The speed of the subject vehicle at the end of the reaction time, $v_n(t+\tau)$, is calculated according to one of these values, whichever governs the situation. The first one is based on the desired speed of the driver, which should not be exceeded. This value becomes competitive with the others, only if the subject vehicle's front is open without any leader (like, after passing the leader). The second one is the basic following (1) if the leader and the follower are in line. For the third one, the speed of the leading vehicle and the MES value are the main constraints in the inequality given by (6). The fourth constraint is the speed value calculated by (11), in which t_{veer} is the time needed to implement the necessary lateral displacement in case of a sudden stop of the leader.

Having calculated $v_n(t+\tau)$, the longitudinal position of the subject vehicle at the end of the reaction time is determined by dynamics as

$$y_n(t+\tau) = y_n(t) + \{v_n(t) \times \tau\} + \frac{1}{2}\frac{v_n(t+\tau) - v_n(t)}{\tau}\tau^2. \tag{13}$$

From the technical specifications of car manufacturers, an average value for the maximum accelerations of vehicles was obtained and compared with earlier similar simulation studies, like Gipps et al. (1980), Gipps (1981) and Benekohal and Treiterer (1988). For the average maximum acceleration capability value, the choice of Gipps (1981) was thought to be the most appropriate. He used a normal distribution with 1.7 m/s^2 mean and 0.3 m/s^2 standard deviation. Similarly, from the same sources, a value of "maximum acceleration multiplied by −2.0" was chosen as the best formulation of maximum deceleration capability of a vehicle. For convenience, τ(reaction time) was chosen as the same as the length of the update steps, i.e. 0.667 s.

4.2. Results

First of all, space–time diagrams of follower–leader pairs were drawn for various frictional clearances (Fig. 12). In these graphs FC = (ERW – width of follower)/2.0 is taken. Vehicular characteristics, like desired speeds, maximum acceleration rates, etc. for the two leaders were set to be equal to each other, so that these two vehicles move together. The follower was released at a higher speed, i.e. 90 km/h, and eventually met these two vehicles travelling at 30 km/h. It is clear from the diagrams that for the FC value 0.5 m, the subject vehicle prefers to follow these two leaders, rather than passing through them. Since the possibility of a lateral shift is eliminated in this experiment, the only constraint in the car following equation was MES. The elimination of the veering constraint by programming around it was on purpose, so that in effect the experiment was a test of the reasonableness of the escape route constraint. It is quite reasonable that to pass through these two vehicles is rejected, because such a passage with these narrow clearances would not be practical at the speed of around

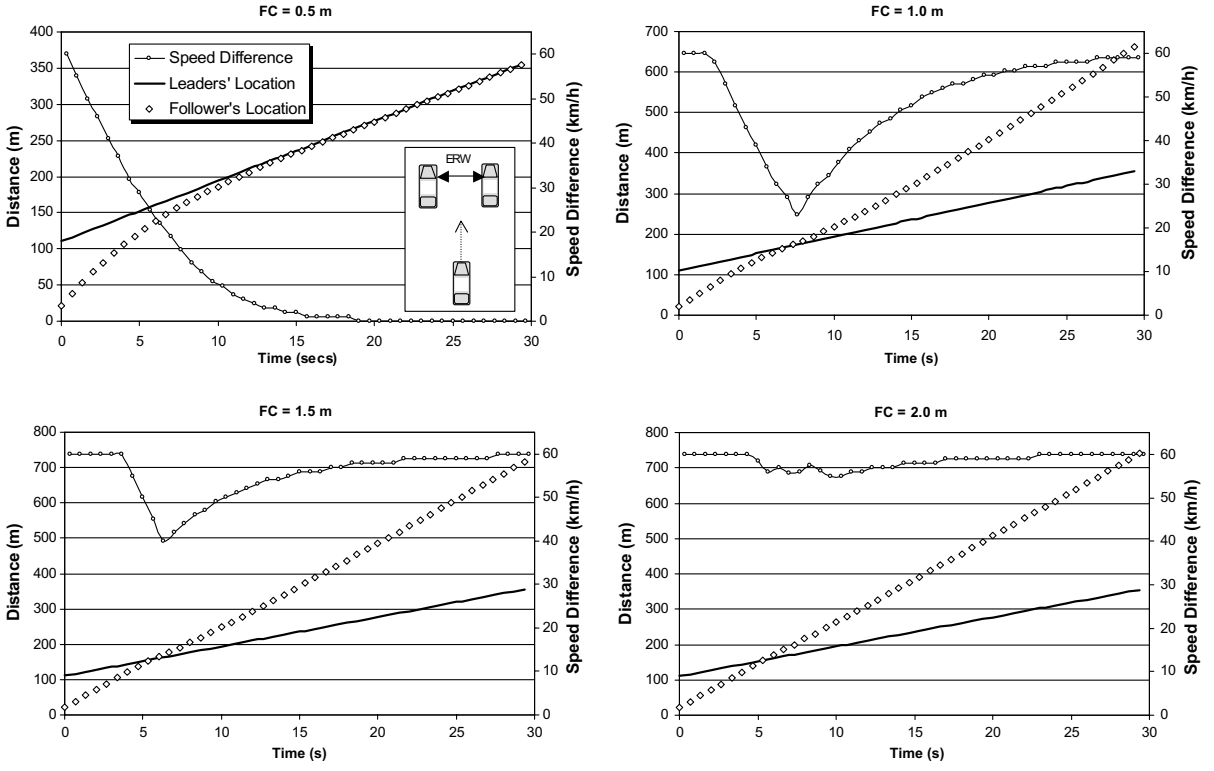

Fig. 12. Simulated trajectories of a vehicle approaching at 90 km/h with various ERWs. The speed difference between the follower and its leader is given on the secondary y-axis on the right.

30 km/h. Since the slopes of the location curves in the diagrams are in fact the speeds of vehicles, it is clearly observable that when FC values were greater than 0.5 m, the subject vehicle exhibits some slowing down during passing. This, too, results from the new car following formula. For the FC values greater than 0.5 m, after the passing, the subject vehicle's movement is not restricted by these vehicles, and hence the subject vehicle is no longer a follower. Note that this amount of lateral clearance (i.e. about 4.0 m, assuming that the width of the approaching vehicle is 1.5 m) provides more or less the same opening as a standard highway's lane widths do. The curve in the fourth graph showing slight hesitation during passing may be interpreted as looming effect of the two vehicles on the speed of the subject vehicle. In general, when the state is stable a smooth trend in the speed curve is observed. When some deceleration/acceleration is required, small fluctuations in the speed curve took place. It should also be noted that since the speeds of the leaders were set constant, these fluctuations belong to the follower.

In the second experiment, the simulation was run five times for five different random seed numbers (Fig. 13) to choose random values for parameters like acceleration, deceleration, vehicle widths/lengths, desired speeds, etc. In order to see the effect more clearly, the speeds of the leaders are controlled at 30 and 50 km/h in these figures, respectively. The speed of the follower, obviously, is calculated by the simulation as a result of the prevailing car following and friction criteria. In both figures, it can be observed that with increasing width of the travel path of the following vehicle, the speed of the following vehicle also increased. When FC values were less than around 0.5 m, no results were obtained, meaning no passing took place, i.e. the follower preferred to follow the leaders. When the FC values were more than around 1.5 m, speeds seemed to be unaffected.

Thirdly, the space–time-speed diagrams are also drawn for various central separations (Fig. 14). When there is only one leader, and the follower is not situated on the edge of the carriageway, there will not be an escape route, and hence no MES restrictions exist. Therefore, the governing factor in the calculation of the follower's movements will be the amount of the off-centredness between these vehicles (t_{veer} constraint).

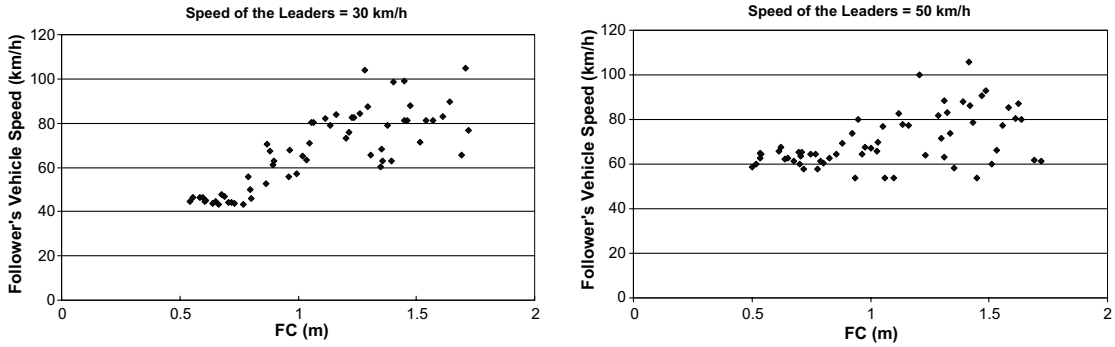

Fig. 13. Simulated relationship between frictional clearances (FC) and passing speeds.

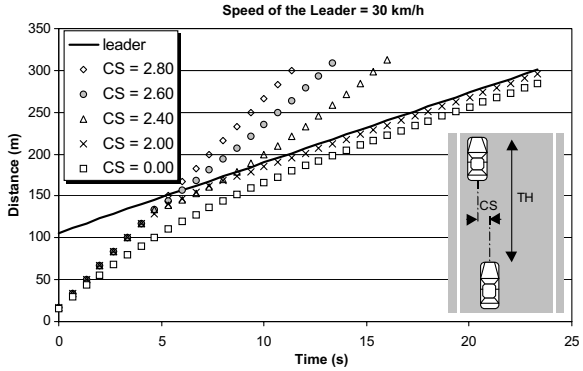

Fig. 14. Simulated trajectories of a vehicle approaching at 90 km/h to its leader travelling at 30 km/h, with various centreline separations (CS).

According to the results, when CS is smaller than 2 m, the interaction is a basic car following case. When it is between 2 and 2.6 m, a staggered car following takes place. When the lateral separation between the two vehicles is 2.8 m or greater no car following interaction is observed.

The vertical distance between the trajectory curves in the space–time diagrams is, as one expects, the longitudinal distance between the geometrical centres of the follower and its leader. Besides, each curve represents only a single run of the simulation. When the following headways are of concern, a slightly modified output was required (Fig. 15). In order to reflect the stochastic nature of the phenomenon, for each 10 cm increment of CS, the simulation was run five times for five different random seed numbers. The diagrams show the declin-

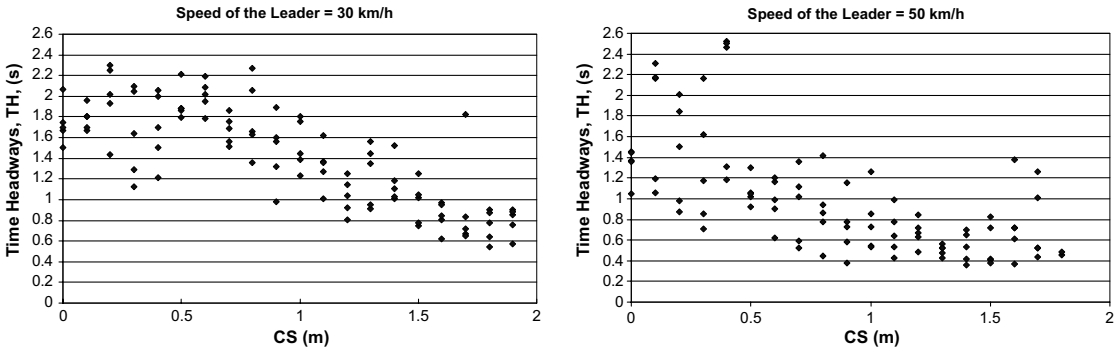

Fig. 15. Simulated relationship between the central separations of consecutive vehicles and the time headway between them.

ing relationship between CS and time headways. As a matter of fact, this trend was earlier observed empirically based on the data mentioned in Section 1 and showed that for CS values of 0.0 m, 1.0 m, and 2.0 m, TH values were around 1.2 s, 1.0 s, and 0.6 s, respectively. Although the simulation results are a bit more conservative in terms of safe following headways, they agreed on a decreasing pattern.

5. Concluding remarks

The major contribution of this paper comes from its recognition of lateral discomfort in car-following, an issue that was not (fully) treated in the past. Existing car following theories may not be applicable in certain cases due to some of the assumptions they possess. For instance, each vehicle is expected to be influenced directly by the one in front, which can only happen where lane discipline is extremely perfect and road/traffic conditions are ideal. However in many real-world situations, even in developed countries, lateral clearances for vehicles change all the time. Examples include: variations in lane widths, existence of street furniture, heterogonous traffic compositions (leading to the variations in vehicle widths) and poor pavement surfaces (drivers deviating from the travelled path to avoid pot-holes). All of these factors may have implications on capacity, speed, and safety. Thus, this feature of traffic flow cannot be negligible and it must be quantified and included in microscopic traffic models for better accuracy. Software that is marketed in developing countries should be particularly concerned with this issue, since the scale of this problem is much bigger in those places. Therefore, further research was worth undertaking, and a new car following model taking into account lateral frictions between vehicles was developed. This incorporation of lateral friction offers a potential breakthrough in the fields of car-following theory and microscopic traffic simulation. It can also potentially influence highway capacity and level of service computation. Upon the completion of tests, the model may be more suitable for cases where the lateral distribution of traffic exhibits irregularities. The simulation results presented in the paper and their verification were obtained from the special runs of the program where the vehicular interactions were treated microscopically in isolation. The validation of the model can only be achieved by simulating a stream of traffic together with all other elements, such as lane changing manoeuvres or with various traffic compositions. It requires obtaining results including flow, speed and density characteristics. Regarding these concerns, on one hand, examination of the correlation between full-scale empirical data and simulation might be complex, and this will be the challenge of future work to be discussed elsewhere. But, on the other hand, in addition to the longitudinal interactions of simulated vehicles, the model takes the lateral positions of vehicles into account. Thus, compared to the previous car following theories, the present work mimics two-dimensional interactions for better realism in modelling.

Acknowledgements

The author thanks Professor Michael G. Bell, Imperial College London, for his comments. The Traffic Laboratory at the University of Newcastle upon Tyne and the Audio Visual Services of the University of Ulster are also acknowledged.

Appendix A

From dynamics, the distance travelled by a decelerating object is formulated as $v(\Delta t) - \frac{1}{2}b(\Delta t)^2$ where v is the speed of the vehicle, b is the rate of change of speed with respect to time and Δt is the time change. In our case $b = \frac{v-\mathrm{MES}}{\Delta t}$ and $\Delta t = \frac{v-\mathrm{MES}}{b}$. By substituting this into the distance formula above, we obtain $v\left(\frac{v-\mathrm{MES}}{b}\right) - \frac{1}{2}b\left(\frac{v-\mathrm{MES}}{b}\right)^2$. After tidying this up, it becomes $\frac{v^2-\mathrm{MES}^2}{2b}$ or $-\frac{\mathrm{MES}^2-v_n^2(t+\tau)}{2b_n}$ for convenience.

Appendix B

The accuracy of the derivation of the proposed model may be checked by using numeric values. For example, for

$b_n = 2\ \text{m/s}^2$,
$b_{n-1} = 2.5\ \text{m/s}^2$,
$\tau = 0.667\ \text{s}$,
$v_n(t) = 20\ \text{m/s}$,
$v_{n-1}(t) = 15\ \text{m/s}$,
$\text{MES} = 8\ \text{m/s}$,
$y_n(t) = 25\ \text{m}$,
$y_{n-1}(t) = 75\ \text{m}$, and
$s_{n-1} = 6\ \text{m}$,

according to (6), a positive root should be

$$v_n(t+\tau) \leqslant 2 \times 0.667 + \sqrt{(2 \times 0.667)^2 + 4\left(20 \times \frac{0.667}{2} + \frac{8^2}{4} + \frac{15^2}{5} + 25 - 75 + 6\right)}$$

$$v_n(t+\tau) \leqslant 11.1554\ \text{m/s},$$

and (5) should yield 0.0 for this value as shown below.

$$-\frac{11.155^2}{4} + 0.667 \times 11.155 + \frac{0.667}{2}20 + \frac{8^2}{4} + \frac{15^2}{5} + 25 - 75 + 6 = 0.0.$$

Appendix C

The following calculations compare Gipps' Model, (1), and a special case of the proposed model, (6). For example, for the same input parameters given in Appendix B, except for $b = 2.5\ \text{m/s}^2$ (b was explained in Section 2), and $\text{MES} = 0\ \text{m/s}$, (1) yields

$$v_n(t+\tau) \leqslant 2 \times 0.667 + \sqrt{2^2 \times 0.667^2 - 2 \times \left\{2 \times (75 - 6 - 25) - 20 \times 0.667 - \left(\frac{15^2}{2.5}\right)\right\}},$$

$$v_n(t+\tau) \leqslant 7.031\ \text{m/s},$$

and (6) gives the same figure:

$$v_n(t+\tau) \leqslant 2 \times 0.667 + \sqrt{(2 \times 0.667)^2 + 4\left(20 \times \frac{0.667}{2} - 0.0 + \frac{15^2}{5} + 25 - 75 + 6\right)},$$

$$v_n(t+\tau) \leqslant 7.031\ \text{m/s}.$$

References

Benekohal, R.F., Treiterer, J., 1988. CARSIM: car-following model for simulation of traffic in normal and stop-and-go conditions. Transportation Research Record 1194, 99–111.
Brackstone, M., McDonald, M., 1999. Car-following: a historical review. Transportation Research Part F 2 (4), 181–196.
Case, H.W., Hulbert, S.F., Mount, G.E., Brenner, R., 1953. Effect of a roadside structure on lateral placement of motor vehicles. Highway Research Board 32, 364–370.
Daganzo, C.F., 2006. In traffic flow, cellular automata = kinematic waves. Transportation Research Part B 40 (5), 369–403.
Forbes, T.W., 1963. Human factor considerations in traffic flow theory. Highway Research Record (15), 60–66.
Gipps, P.G., 1981. A behavioural car following model for computer simulation. Transportation Research Part B (15), 105–111.
Gipps, P.G., Wilson, B.G., 1980. MULTSIM: a computer package for simulating multi-lane traffic flows. In: Proceedings of the fourth Biennial Conference, Australia, pp. 88–93.
Gunay, B., 2003. Methods to quantify the discipline of lane-based driving. Traffic Engineering and Control 44 (1), 22–27.
Gunay, B., 2004. An investigation of lane utilisation on Turkish highways. ICE-Transport Journal 157 (1), 43–49.
Highway Capacity Manual, 2000. Transportation Research Board National Research Council.

Holland, E.N., 1998. A generalised stability criterion for motorway traffic. Transportation Research Part B 32 (2), 141–154.
Khan, S.I., Maini, P., 1999. Modelling heterogeneous traffic flow. Transportation Research Record 1678, 234–341.
Leutzbach, W., Wiedemann, R., 1986. Development and applications of traffic simulation models at the Karlsruhe Institut fur Verkehrwessen. Traffic Engineering and Control 27 (5), 270–278.
Mahalel, D., 1984. Appraisal of traffic stream friction. Transportation Research Part A 18 (3), 225–230.
Martens, M., 1997. The effects of road design on speed behaviour: a literature review. MASTER. The European Commission under the Transport RTD Programme of the fourth Framework programme. Deliverable D1. University of Leeds, UK.
May, A.D., 1959. A friction concept of traffic flow. Highway Research Board, Washington DC, pp. 493–509.
May, A.D., 1990. Traffic Flow Fundamentals. Prentice Hall, New Jersey.
Michales, R.M., Cozan, L.W., 1963. Perceptual and field factors causing lateral displacement. Public Roads 32 (11), 233–240.
Nagel, K., Schreckenberg, M., 1992. J Physique I 2 (221).
Pipes, L.A., 1966. Car following models and the fundamental diagram of road traffic. Transportation Research 1 (1), 21–29.
Taragin, A., 1955. Driver behaviour as affected by objects on highway shoulders. Highway Research Board 34, 453–472.